Camera-based forecasting of insolation for solar systems

Daniel Manger, Frank Pagel

Fraunhofer Institute of Optronics, System Technologies and Image Exploitation (IOSB),
Fraunhoferstr. 1, 76131 Karlsruhe, Germany

ABSTRACT

With the transition towards renewable energies, electricity suppliers are faced with huge challenges. Especially the increasing integration of solar power systems into the grid gets more and more complicated because of their dynamic feed-in capacity. To assist the stabilization of the grid, the feed-in capacity of a solar power system within the next hours, minutes and even seconds should be known in advance. In this work, we present a consumer camera-based system for forecasting the feed-in capacity of a solar system for a horizon of 10 seconds. A camera is targeted at the sky and clouds are segmented, detected and tracked. A quantitative prediction of the insolation is performed based on the tracked clouds. Image data as well as truth data for the feed-in capacity was synchronously collected at one Hz using a small solar panel, a resistor and a measuring device. Preliminary results demonstrate both the applicability and the limits of the proposed system.

Keywords: camera, forecast, feed-in capacity, solar systems, clouds, insolation, tracking.

1. INTRODUCTION

Integrating the energy from renewable energy sources into the grid gets increasingly challenging for the electricity suppliers. In particular, the volatile output of solar power systems is a problem since due to clouds in front of the sun the output can drop within seconds to a fraction of maximum feed-in capacity. While flexible energy storages for short-term surpluses are still a research topic, there are also initiatives to control the feed-in capacity. For example, in Germany, new solar power systems have to be equipped with functionalities for remote shut-down so that grid operators can limit or even shut down solar power systems in case of grid overloads. Since according to current law, the owners of the solar power systems have to be reimbursed for the lost feed-in compensation, this leads to the absurd situation that ultimately, the end-consumers are paying for the unused power, too. To solve the problem by dynamic energy storages and for the proper stabilization of the grid, the feed-in capacity of a solar power system within the next seconds, minutes and hours should be known in advance. Coarse predictions are possible with the information of the weather forecast or from satellite images. However, both the temporal and the spatial resolution of satellite images are not sufficient for an accurate short-term forecast for one system at a certain location. Therefore, in recent years, considerable research has been spent in the domain of camera-based prediction systems for such short-term forecasts.

2. RELATED WORK

Using ground-based camera images to obtain information about cloud characteristics has attracted more and more attention in recent years. Estimating the cloud coverage[1–3] in the sky or classifying cloud types[2–5] are some examples. Forecasting the solar insolation is another important application which has been addressed with various input sources such as weather forecasts, satellite-based cloud images, time series analysis, distributed insolation sensors or other data from connected photovoltaic systems in the neighborhood. Predictions of the future insolation based on the positions and speed of the clouds in a current camera image is another important source of information which can have advantages in both temporal and spatial accuracy. [1] work with the Total Sky Imager (TSI) capturing two images per

minute at low resolution. They focus on the propagation of the cloud field by a global velocity vector and evaluate matching errors compared to the future image. With a different model of the TSI, [6] capture one image per minute at a resolution of 352x288 and calculate also one global velocity vector for all clouds. Depending on its orientation and magnitude, six grid cells in the image are defined assuming to contain the cloud pixels which are responsible for the direct normal irradiance (DNI) forecasts for time horizons of 3 to 15 minutes. Evaluations are presented comparing the forecasts with the DNI and with the persistence model. The most significant forecast accuracy is reported to be possible for 5 minutes ahead. [7], [8] work with a sun-tracking camera at one frame per second and a resolution of 1024x1280. Assuming a constant cloud velocity, the arrival time up to 10 minutes in advance can be predicted with an accuracy of few minutes. Cloud dynamics such as cloud formation and dissipation are reported to limit the accuracy.

Figure 1: Result of the segmentation of clouds based on a SVM.

This work describes an inexpensive camera-based insolation forecasting system. The focus of the forecast is on days where clouds of the type cumulus and stratocumulus cover the sun for several seconds up to some minutes. To predict even the short-term drops in insolation of several seconds, the system operates at one Hz, i.e. each second, the current image is analyzed and a new forecast is calculated. Please note, that this is an important difference in contrast to many existing works which operate at one [6] or two [1] samples per minute and aim at a forecast horizon of up to 15 minutes [1], [6–8]. Especially, in weather situations where clouds of relevant size are formed and clouds merge, split or vanish within one minute, the output of such coarse forecast systems is of limited meaningfulness since, virtually, the sampling theorem is violated.

3. HARDWARE SETUP

For image acquisition, we use a GoPro Hero3 action camera. Being designed for outdoor scenarios, its dynamic range is sufficient to provide proper images even when directly looking into the sun (see Figure 1). The wide field of view of 150° covers a large part of the sun's trajectory. Using a HDMI capturing device, we acquire color images at 1 frame per second with a resolution of 1920x1080. For measuring the solar insolation, we use a small photovoltaic module (10″

diagonal, 12V, 5W) which is connected to a 40Ω resistor. The electric current of the circuit is logged synchronously with every image and is between 50 mA and 300 mA. Data has been acquired in Karlsruhe and Ilmenau, Germany in August and September 2014. Please note, that this is a rather inexpensive hardware setup compared to other systems working with sun-tracking cameras with elements to actively obscure the sun's position in the image [1], [6–9].
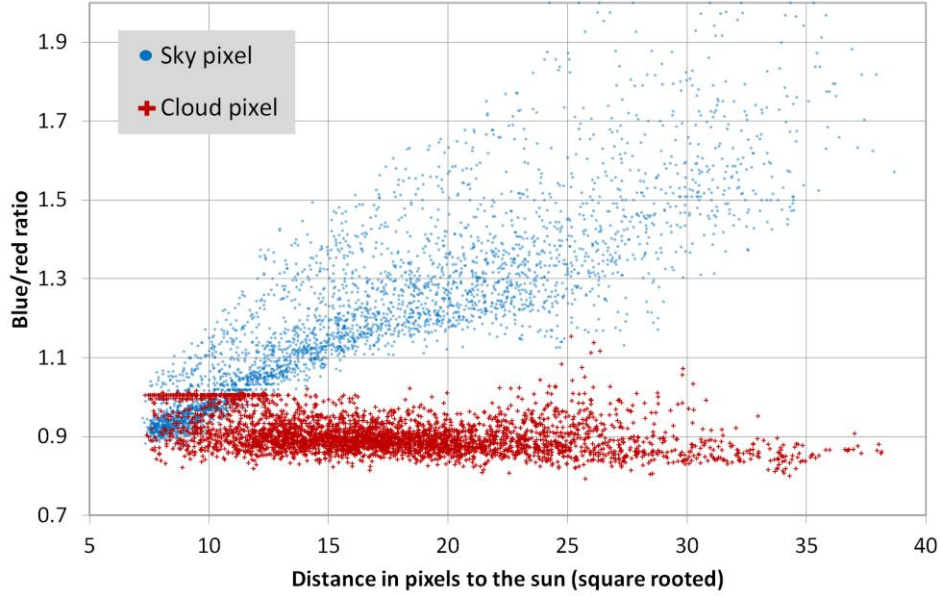

Figure 2: The segmentation of cloud and sky pixels based on a threshold for the blue/red-ratio is not possible in areas close to the sun. The red line-type structure at a blue/red-ratio of 1 originates from frequent white cloud pixels close to the sun.

4. CLOUD DETECTION

For the detection of clouds, we make use of the current position of the sun in the image. Although the position could be calculated by camera calibration and meteorological information, we extract it form the images which is possible if from time to time the sun is not covered by clouds and can be localized in the image. By counting the number of the brightest pixels in the images with $(R + G + B)/3 > 253$ and filtering with a certain range, we select those images where the sun is expected to be clearly visible. The mean x and y positions of the respective pixels are taken as hypotheses for the center of the sun in the respective image. For all hypotheses, a model is fitted using the least-squares method. Amusingly, both the mapping from the time to the x-coordinate as well as the mapping from x to y-coordinate of the sun turned out to be a straight line in our setup. Of course, for different latitudes, times of the year and the camera lenses, a polynomial model might be more appropriate.

The segmentation of image pixels into cloud and sky has been performed in various ways in the literature. Several methods use a global fixed threshold of the ratio[1], [9] or the difference [5] of the red and blue intensities. This is motivated by the fact that in contrast to clear sky, the aerosols, water drops and ice crystals in clouds scatter blue and red light similarly leading to the white or grey appearances of clouds. However, in the area close to the sun, the red/blue ratio histograms for clouds and clear sky overlap as can be seen in Figure 2. Hence, adaptive thresholds have been proposed to find the optimal threshold given the actual distributions in the image, e.g. based on the Otsu algorithm[10] or on the Minimum Cross Entropy (MCE)[2], [4], [6]. Nevertheless, even when using a separate fixed threshold for the red/blue ratio or difference or multicolor criterion[3] for each image, the circumsolar region cannot be segmented correctly and is therefore omitted in many works. However, for a proper short-term forecast, the clouds close to the sun are of the utmost importance because they contain the latest evidence for the forecast.

We therefore propose a learning-based segmentation utilizing a classifier directly incorporating the distance to the sun. More specifically, we annotated 30k pixels in various scenes into cloud or sky pixels and used 80% for training and 20% for testing ensuring that the two sets contain different scenes. Using a support vector machine (SVM) with a radial basis function kernel (RBF), we tested several feature sets. The best result (F-Measure 0.998) was found with a six-

dimensional feature vector integrating red, green and blue intensities, grey-scale values, blue-red differences and the distance to the sun. The latter was square rooted as differences in distances in the circumsolar region are more important than those far away from the sun. For all six dimensions, the input data has been normalized to have zero-mean and unit-variance. For comparison, a linear SVM with just the blue-red differences (representing the fixed global threshold) yielded an F-Measure of 0.865 with a recall of 0.76, i.e. 24% of the cloud pixels could not be detected, many of them being close to the sun. See Table 1 for results of different feature sets and Figure 1 for an example segmentation.

Feature set	SVM	Recall=$\frac{TP}{TP+FN}$	Precision=$\frac{TP}{TP+FP}$	F-Measure=$\frac{2 \cdot Precision \cdot Recall}{Precision+Recall}$
B-R	Linear	0,764	0,998	0,865
B-R, d	RBF	0,947	0,870	0,907
R, G, B	RBF	0,920	0,916	0,918
B-R, R, G, B	RBF	0,967	0,975	0,971
B-R, R, G, B, d	RBF	0,995	0,998	0,996
B-R, R, G, B, d, g	RBF	0,997	0,999	**0,998**

Table 1: Cloud/sky Classification performance for different feature sets: R=red, G=green, B=blue, B-R=blue – red difference, d=distance to the sun, g=grayscale. TP=true positive, FN=false negative, FP=false positive.

5. CLOUD TRACKING

For two subsequent images, the motion of every cloud pixel is estimated by a local bock-based matching. We employ a template matching based on the normalized correlation coefficient in order to cope with the changes in lighting due to the auto-shutter of the camera. As homogeneous regions in middle of the clouds can lead to outliers, we only calculate motion vectors where the local variance of the greyscale pixel intensities is above a threshold. For speedup, the motion vectors are only calculated in a regular grid and interpolated in-between the grid as well as at homogeneous cloud locations where no motion was calculated. To get meaningful motion vectors, we calculate tracks for five subsequent images and exclude tracks which were not stable over the five frames, e.g. because the region became too homogeneous due to disappearing cloud borders. Please note, that in contrast to [1], [6], [8], the tracking is not performed with one global motion vector for all clouds. Instead, the local tracking can handle the many different motion directions for the respective parts of each cloud which is essential for cumulus cloud types. Furthermore, we do not transform the motion vectors with calibration information into global world-coordinates but remain in the image coordinates.

6. INSOLATION FORECAST

Based on the position of the cloud pixels of the current image, we use the motion vectors to generate a forecast for the future position of the cloud pixels in 10 seconds. In an accumulator, we subsequently collect those pixels which are predicted to occlude the sun leading to an area-based coverage with values from 0 (no occlusion at all) to 1 (the sun's area is completely covered). However, since our camera is not equipped with a mechanism to obscure the sun's position in the image, blooming effects can occur. This leads – depending as well on the amount of aerosols, water drops/crystals in the air - to a circular region of some 50 pixel in radius where all pixel intensities are close to the maximum whereas the true radius of the sun is only about 10 pixels. Depending on the speed and on the proximity of a cloud, this lost information in the blooming area can be important for the forecast. We therefore not only use the cloud appearance of the current image but extend the basis of information by incorporating appearances of the last images. More specifically, we use the last 15 images together with their respective motion vectors to predict the cloud pixels into the future. The motion vectors are appropriately scaled to take into account the respective temporal forecast horizon (10 to 25 seconds). For the quantitative insolation forecast, we inversely map the area-based coverage to the minimum and maximum insolation values from the observed data with our system.
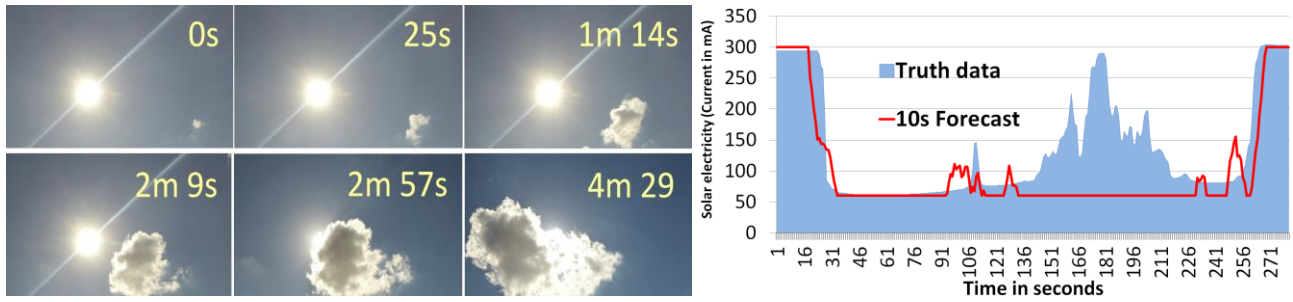
Figure 3: Left: Scene displaying the formation of a cloud (only the relevant cut-out of the FullHD image is displayed). Right: The temporal course of the insolation (blue area) and the 10s forecast (red).

7. RESULTS AND CONCLUSION

Figure 3 shows a typical scene with cumulus clouds. Within one minute, a cloud is formed with a size large enough to completely cover the sun for several seconds. In our setup, after 3 minutes, the cloud starts to impair the insolation for 4 minutes. The example shows that short-term forecasts in dynamic cloud situations with a framerate of one second are challenging. Especially when clouds are segmented into binary masks, the pixels close to the border of a cloud do not properly represent the transparency of the cloud which leads to wrong estimates about the starting and ending time of a shading event. Furthermore, as can be seen in the second half of the sequence, several peaks in the insolation could not be predicted since the insolation depends not only on the area of the sun which is covered but also on the thickness of the involved cloud segments. We therefore plan to adapt the shading model to integrate the thickness of the clouds analyzing the pixel color information of the past frames.

8. REFERENCES

[1]   C. W. Chow, B. Urquhart, M. Lave, A. Dominguez, J. Kleissl, J. Shields, and B. Washom, "Intra-hour forecasting with a total sky imager at the UC San Diego solar energy testbed," *Solar Energy*, vol. 85, no. 11, pp. 2881–2893, 2011.

[2]   Q. Li, W. Lu, and J. Yang, "A hybrid thresholding algorithm for cloud detection on ground-based color images," *Journal of atmospheric and oceanic technology*, vol. 28, no. 10, pp. 1286–1296, 2011.

[3]   P. Tzoumanikas, A. Kazantzidis, A. Bais, S. Fotopoulos, and G. Economou, "Cloud Detection and Classification with the Use of Whole-Sky Ground-Based Images," in *Advances in Meteorology, Climatology and Atmospheric Physics*, Springer, 2013, pp. 349–354.

[4]   E. Gribkoff, S. Park, L. Shigetoshi, and A. Subedy, "Cloud Recognition in the Miami Skyline."

[5]   A. Heinle, A. Macke, and A. Srivastav, "Automatic cloud classification of whole sky images," *Atmospheric Measurement Techniques Discussions*, vol. 3, no. 1, pp. 269–299, 2010.

[6]   R. Marquez and C. F. Coimbra, "Intra-hour DNI forecasting based on cloud tracking image analysis," *Solar Energy*, vol. 91, pp. 327–336, 2013.

[7]   V. T. Jayadevan, J. J. Rodriguez, V. P. Lonij, and A. D. Cronin, "Forecasting solar power intermittency using ground-based cloud imaging," in *World Renewable Energy Forum 2012*, 2012.

[8]   V. P. Lonij, V. T. Jayadevan, A. E. Brooks, J. J. Rodriguez, K. Koch, M. Leuthold, and A. D. Cronin, "Forecasts of PV power output using power measurements of 80 residential PV installs," in *Photovoltaic Specialists Conference (PVSC), 2012 38th IEEE*, 2012, pp. 3300–3305.

[9]   C. N. Long, J. Sabburg, J. Calbó, and D. Pagès, "Retrieving cloud characteristics from ground-based daytime color all-sky images," *Journal of Atmospheric and Oceanic Technology*, vol. 23, no. 5, pp. 633–652, 2006.

[10]   N. Otsu, "A threshold selection method from gray-level histograms," *Automatica*, vol. 11, no. 285–296, pp. 23–27, 1975.